Published in final edited form as:
Dev Dyn. 2008 November ; 237(11): 3128–3141. doi:10.1002/dvdy.21717.

Diverse Roles of E-Cadherin in the Morphogenesis of the Submandibular Gland: Insights Into the Formation of Acinar and Ductal Structures

Janice L. Walker[1], **A. Sue Menko**[1], **Sheede Khalil**[2], **Ivan Rebustini**[3], **Matthew P. Hoffman**[3], **Jordan A. Kreidberg**[4], and **Maria A. Kukuruzinska**[2,*]

[1] Department of Pathology, Anatomy and Cell Biology, Thomas Jefferson University, Philadelphia, Pennsylvania [2] Department of Molecular and Cell Biology, Boston University School of Dental Medicine, Boston, Massachusetts [3] Matrix and Morphogenesis Unit, Craniofacial Developmental Biology and Regeneration Branch, National Institute for Dental and Craniofacial Research, National Institutes of Health, Bethesda, Maryland [4] Department of Pediatrics, Harvard Medical School, Boston, Massachusetts

Abstract

The formation of acinar and ductal structures during epithelial tissue branching morphogenesis is not well understood. We report that in the mouse submandibular gland (SMG), acinar and ductal cell fates are determined early in embryonic morphogenesis with E-cadherin playing pivotal roles in development. We identified two morphologically distinct cell populations at the single bud stage, destined for different functions. The outer layer of columnar cells with organized E-cadherin junctions expressed the neonatal acinar marker B1 by E13.5, demonstrating their acinar fate. The interior cells initially lacked distinct E-cadherin junctions, but with morphogenesis formed cytokeratin 7 (K7) -positive ductal structures with organized E-cadherin junctions and F-actin filaments. Inhibition of E-cadherin function with either siRNA or function blocking antibody caused extensive apoptosis of ductal cells and aberrantly dilated lumens, providing the first evidence that E-cadherin regulates ductal lumen formation during branching morphogenesis of the salivary gland.

Keywords

E-cadherin; submandibular gland; branching morphogenesis; acinar precursors; presumptive ducts; cytodifferentiation; catenins; adherens junctions

INTRODUCTION

Interactions between neighboring cells are central to the morphogenetic changes that guide eukaryotic tissue remodeling and differentiation (Jamora and Fuchs, 2002; Gumbiner, 2005). In epithelial tissues, these interactions are mediated, for the most part by, E-cadherin, a member of the type I classical cadherin family. E-cadherin is a single span transmembrane protein consisting of 5 extracellular cadherin repeats (EC domains) and a short cytoplasmic domain that associates with members of the catenin family. E-cadherin forms calcium-dependent

*Correspondence to: Maria A. Kukuruzinska, Department of Molecular and Cell Biology, Boston University Medical Center, 715 Albany Street, E428, Boston, MA 02118. E-mail: mkukuruz@bu.edu.

Additional supporting information may be found in the online version of this article.

homotypic cell–cell adhesion structures known as adherens junctions (AJs) that mediate intercellular adhesion through dynamic interactions with the actin cytoskeleton (Hirano et al., 1987). In addition to providing intercellular adhesion, AJs regulate cell polarity, cell–cell communication, cell survival, cell differentiation, and tissue development (Grunwald, 1993; Marrs and Nelson, 1996; Wheelock and Johnson, 2003; Halbleib and Nelson, 2006). AJs provide instructive signals in the morphogenetic processes by which an epithelial sheet forms a specialized three-dimensional structure (Takeichi, 1991; Nakagawa and Takeichi, 1995; Jamora and Fuchs, 2002; Gumbiner, 2005; Halbleib and Nelson, 2006). Furthermore, AJs function in the establishment and maintenance of differentiated tissue architecture (Gumbiner, 1996, 2005; Wheelock and Johnson, 2003; Halbleib and Nelson, 2006).

The submandibular gland (SMG) belongs to a group of epithelial tissues that develop through a series of morphogenetic changes collectively referred to as branching morphogenesis (Bernfield et al., 1984; Hieda and Nakanishi, 1997; Fernandes et al., 1999; Jaskoll and Melnick, 1999; Patel et al., 2006). The SMG has long been regarded as a model for branching morphogenesis, and in recent years it has become a valuable tool for the identification of key regulators and molecular mechanisms underlying this developmental process. In particular, the ability to grow early embryonic SMGs in organ culture, an ex vivo system that closely reproduces in vivo branching morphogenesis, has proven instrumental to the unraveling of some aspects of this process (Kashimata et al., 2000; Sakai et al., 2003). In the mouse, SMG development begins at embryonic day 11 (E11) as an epithelial thickening that gives rise to the initial bud structure by E12.5. The initial bud subsequently grows and undergoes rounds of clefting and new bud formation leading to extensive branching into the surrounding mandibular mesenchyme. As morphogenesis progresses, regions of the branching epithelium undergo cytodifferentiation, eventually giving rise to a tree-like structure consisting of differentiated terminal secretory units, the acini, and an array of secondary ducts that empty into the principal excretory duct and ultimately into the oral cavity (Denny et al., 1997; Jaskoll and Melnick, 1999; Patel et al., 2006).

To date, several studies have shown a pivotal role for E-cadherin in salivary gland morphogenesis. Disruption of E-cadherin cell– cell adhesion by modulating Rac function in Drosophila interfered with proper salivary gland development (Pirraglia et al., 2006). Recent studies in which SMG buds were reconstructed from isolated SMG cells provided evidence that E-cadherin junctions contributed to the structural organization of the gland and its ability to undergo branching morphogenesis (Wei et al., 2007). Therefore, an in depth knowledge of how E-cadherin-mediated adhesion impacts SMG development will have important implications for the general understanding of epithelial tissue development through branching morphogenesis.

We have undertaken detailed analyses of E-cadherin and its junctional proteins' localization and actin cytoskeletal association from the initial bud stage through embryonic cytodifferentiation using high-resolution confocal microscopy imaging. Moreover, we have investigated the functional significance of E-cadherin during early morphogenesis using both an E-cadherin function blocking antibody and partial silencing of E-cadherin expression with siRNA. Our findings show that as early as the initial bud stage, the E12.5 SMG contains two morphologically distinct cell populations with different E-cadherin junctional organization and functional outcomes for development. The outer cell layer in contact with the basement membrane consists of closely packed epithelial cells that surround polymorphous cells located in the inner bud region. Such a cellular organization has been reported only for later stages of SMG morphogenesis based on electron microscopy studies (Kadoya and Yamashina, 1989, 1993; Kadoya et al., 1995). We provide evidence that already in the initial bud the outer peripheral cells had well-organized E-cadherin junctions. By E13.5, these cells expressed a biochemical marker of neonatal acinar cell differentiation, demonstrating that acinar cells are

determined very early in SMG development. Our findings that cytoarchitecture and intercellular junctions characteristic of columnar acinar cell morphology are established in the peripheral layer at the initial bud stage suggests that commitment to the acinar lineage may occur at or prior to these earliest stages of SMG development. In contrast, the cells in the inner bud region have less-defined E-cadherin junctions and express duct-specific markers, suggesting that they are destined to form ductal structures. Importantly, our studies demonstrate that E-cadherin provides a survival signal to duct cells during lumen formation. Moreover, E-cadherin is required for the branching morphogenesis and outgrowth of the developing SMG. Collectively, our studies define distinct developmental roles for E-cadherin in the formation of acinar and ductal structures during SMG branching morphogenesis.

RESULTS

SMG Organ Culture

The SMG develops through branching morphogenesis from an epithelial bud into an array of ducts terminating in secretory acini (Denny et al., 1997; Jaskoll and Melnick, 1999; Patel et al., 2006). Studies of SMG embryonic development have been facilitated by its ability to undergo branching morphogenesis and cytodifferentiation in organ culture. Under ex vivo conditions, the temporal and spatial aspects of SMG morphogenesis have been shown to resemble the in vivo events (Patel et al., 2006). In the present work, we elected to use SMG organ cultures from the initial bud at E12.5 until the completion of embryonic cytodifferentiation at E18.5 (Fig. 1).

Identification of Acinar and Ductal Cell Precursors

Distinct cell populations in the SMG undergoing morphogenesis—Little is known about the mechanisms underlying the branching morphogenesis of epithelial tissues and the formation of acinar and ductal structures in the embryonic SMG, in particular. To gain insights into how these functional units are formed, we examined cells in the developing SMG by staining for filamentous actin (F-actin) that delineates the cytoarchitecture of the cells within this tissue. As early as the initial SMG bud stage (E12.5), localization of F-actin revealed a unique population of cells with columnar morphology that lined the bud's periphery (Fig. 2A, solid box, B, block arrow) and was in contact with the basement membrane (Fig. 2J). This peripheral cell population with columnar morphology surrounded a group of rounded cells in the bud's interior (Fig. 2B, open arrow). Previous studies have shown that at the single bud stage, the majority of cells were highly proliferative, with the exception of cells located in the most proximal region of the SMG stalk (Supp. Fig. 1A, which is available online) that becomes the main duct of the gland (Melnick and Jaskoll, 2000). This is the first demonstration that two distinct cell populations exist at the single bud stage. Importantly, the outer cell layer with columnar morphology was maintained throughout embryonic development (E13.5, Fig. 2D, solid box, E, block arrow), although there were distinct changes in the shape and packing of these cells as the SMG developed.

We next sought to determine the fate of cells in the outer layer. Although to date no markers for acinar cell progenitors have been described, expression of B1-immunoreactive proteins (B1) has been associated with neonatal acinar cells in the SMGs of rat and mouse (Mirels et al., 1998; Ball et al., 2003). To determine whether cells of the outer peripheral layer were committed to the acinar lineage early in SMG development, we examined SMGs from the single bud stage for expression of B1. While at E12.5 no B1-specific immunostaining was detected (Fig. 2A–C), high levels of B1 were expressed and restricted to the outer columnar cell layer by E13.5 (Fig. 2D, white solid box; E, block arrow). This pattern of B1 expression in the peripheral layer was maintained throughout SMG morphogenesis (E15.5; Fig. 2G) with B1 being expressed only by acinar cells in the cytodifferentiated SMG (E18.5; Fig. 2H).

Immunostaining for Ki67, a proliferation marker that stains nuclei, showed that these peripheral columnar cells remained proliferative following their commitment to the acinar lineage (Supp. Fig. 1B). Western blot analyses of SMG protein extracts showed detectable levels of B1-immunoreactive protein(s) (25 kDa) as early as E13.5 that increased dramatically in abundance in the cytodifferentiated E18.5 SMG (Fig. 2I). Collectively, our results suggest that acinar cell precursors are present in the outer layer already at the single bud stage. In addition, these studies strongly support a model in which the outer layer of the early SMG is the source of acinar structures in cytodifferentiated glands (Fig. 2K, model).

Our B1 immunolocalization results provide the first demonstration of early expression of an acinar cell marker in the outer cell layer that we now know is destined to develop into acini. We also examined the distribution of aquaporin 5 (AQ5) in the early developing SMG, a water channel protein expressed by both intercalated ducts and acini. Transcripts for this functional marker are expressed at E15 (Wei et al., 2007). Low level of immunostaining for AQ5 was observed at E15.5 in the newly forming ducts, but not in the outer cell layer (Supp. Fig. 2). At late stages of embryonic development (E18.5), AQ5 was prominently localized to the apical membranes of acinar structures and intercalated ducts (Supp. Fig. 2). These results emphasize the importance of B1 protein as the earliest marker of cells destined to become acini.

In contrast to the columnar cells in contact with the basement membrane in the acinar progenitor layer, F-actin staining revealed that at the single bud stage, interior cells were rounded (Fig. 2B, open arrow). By E13.5, cells in the proximal regions of the terminal buds had undergone dramatic morphogenetic changes to form early ductal structures (Fig. 2D,F). These cells were prominently stained with fluorescence-conjugated phalloidin, which revealed the early organization of cortical actin structures we previously showed to be characteristic of mature SMG ducts (Menko et al., 2002). At this early stage of development, F-actin staining demonstrated prominent extensions of the newly forming ducts leading to the inner bud regions (Fig. 2D, detailed in Supp. Fig. 3A), which overlapped with staining for the duct specific marker cytokeratin 7 (K7) (Yamaguchi et al., 2006) even prior to the appearance of ductal lumens (Fig. 3, Supp. Fig. 3B). These results provide evidence that proximal regions of the terminal buds were sites of presumptive duct formation. In cytodifferentiated SMGs at E18.5, F-actin delineated acinar lumens that were directly connected to ductal structures (Suppl. Fig. 3C). Thus, while the outer peripheral cells were acinar cell precursors, the inner cells of the SMG epithelial bud formed ductal structures. These data provide a new paradigm for the extension of ductal structures during branching morphogenesis of the SMG.

Organization of E-cadherin junctions in distinct cell populations—The organization of E-cadherin junctions during SMG morphogenesis was investigated by immunolocalization analysis of E-cadherin and its associated junctional proteins α-, β-, and γ-catenin. From the initial bud stage, E12.5, E-cadherin, and β-catenin, a principal cadherin binding partner, were localized to the lateral surfaces of the columnar cells that comprised the outer layer (Fig. 4B,C block arrows). At this early stage of development, staining for E-cadherin and β-catenin in the interior cells was diffuse (Fig. 4B,C open arrows) indicating that they had less organized E-cadherin junctional structures. As the acinar progenitor layer continued to expand (E13.5) and undergo cytodifferentiation (E18.5), tightly focused staining for E-cadherin and β-catenin was maintained (Fig. 4G,H,L,M). To identify the acinar structures in cytodifferentiated SMGs, glands at E18.5 were double labeled for F-actin, which at this stage of development delineated the cells' apical membranes facing the acinar lumens (Fig. 4L–O, regions stained red).

In contrast to the localization of E-cadherin and β-catenin at the single bud stage, staining for γ-catenin in the peripheral layer was diffuse, suggesting at this time of development that γ-catenin was not a principal component of E-cadherin junctions (Fig. 4D). Although γ-catenin

staining remained primarily diffuse at E13.5, some cell– cell border localization in the outer layer could be detected (Fig. 4I). On the other hand, in cytodifferentiated acinar cells at E18.5, γ-catenin staining was well focused at cell–cell borders (Fig. 4N). α-catenin, which is both a cadherin junctional component and an actin cross-linker, was localized to cell– cell interfaces in the acinar layer throughout SMG development (Fig. 4E,J,O) with a particularly high concentration in the apical regions of these cells (Fig. 4E,J, broken arrow). This apical distribution of α-catenin was very similar to the localization of F-actin in the peripheral layer (see Fig. 2). Since E-cadherin junctions were present in the peripheral cell layer even prior to detection of the differentiation marker B1, their primary function may be in establishing polarity of acinar precursor cells.

Formation of lumenized ducts was coincident with assembly of E-cadherin junctions at the apicolateral borders of the cells that lined the ductal lumen in the distal region of the initial stalk (Fig. 5A). A similar pattern of localization was detected for β-catenin (data not shown). As reported previously (Heida and Nakanishi, 1997), we observed ZO-1 at the apical domains of the cells that were adjacent to the lumenizing region of the newly formed duct (Fig. 5B), resembling the apical localization of F-actin in these developing structures (Supp. Fig. 3A). Apical localization of ZO-1 is indicative of the presence of tight junctions whose assembly has been shown to be preceded by the formation of stable E-cadherin junctions (Hartsock and Nelson, 2007). Thus, the presence of ZO-1 in cells with well-organized E-cadherin junctions in the newly forming ducts strongly suggests that E-cadherin plays a role in the maturation of these ductal cells. Collectively, our data show distinct organization of E-cadherin junctions in the developing acinar and ductal structures that are likely to play essential roles in their morphogenesis.

Stabilization of E-cadherin junctions accompanies SMG cytodifferentiation—To examine cytodifferentiation-specific changes in the composition of E-cadherin junctional complexes, E-cadherin was immunoprecipitated from SMGs at stages representing early morphogenesis (E13.5) and late cytodifferentiation (E18.5) and analyzed for association with catenins, the major components of adherens junctions, by immunoblotting (Fig. 6A). Note that β-, γ-, and α-catenin associate with E-cadherin in a mutually exclusive manner (Cowin et al., 1986). The abundance of catenins in complex with E-cadherin at E13.5 was compared to E18.5 after assessing catenin/E-cadherin ratios at E13.5 and expressing them relative to the value at E18.5. While there was little change in the association of β-catenin with E-cadherin between early morphogenesis and late cytodifferentiation, the association of γ- and α-catenin with E-cadherin complexes increased as the gland matured (Fig. 6A). The association of α-catenin with E-cadherin complexes has been shown to be involved in the linkage of these junctions to the actin cytoskeleton. Interestingly, in development, the association of γ-catenin with classical cadherins can mediate the stabilization of these junctions by linking them to the intermediate filament cytoskeleton (Leonard et al., 2008). These results suggest that increased stabilization of the E-cadherin complexes occurred with the formation of mature acini and ducts and that there was greater diversity in the types of E-cadherin junctions in cytodifferentiated glands than during early morphogenesis.

Linkage of cadherin junctions to the Triton-insoluble cytoskeleton has been used as a hallmark of cadherin complex stability (Cowin and Burke, 1996). In a previous study, we demonstrated that at late stages of SMG cytodifferentiation, a high percentage of the total E-cadherin and β-catenin were Triton-insoluble (Menko et al., 2002). Here, we have extended these studies to include early stages of SMG development. Immunoblot analysis of the Triton-solubility of E-cadherin showed that the amount of E-cadherin associated with the Triton-insoluble cell fraction increased greatly from E13.5 to cytodifferentiated SMG (Fig. 6B). This was consistent with the increased linkage of both α- and γ-catenin to E-cadherin junctions at this late developmental stage. This trend was paralleled by β-catenin (Fig. 6B). Triton solubility of α-

catenin was unaltered during SMG embryonic development (Fig. 6B), most likely reflecting the multiple roles that α-catenin plays in the cell, including as one of the cross-linkers of actin filaments (Kobielak and Fuchs, 2004; Benjamin and Nelson, 2008). Much of the increased Triton-insolubility of E-cadherin was likely to be related to its association with γ-catenin, which also became highly insoluble at E18.5. This is consistent with the localization of γ-catenin to cell–cell interfaces at late developmental times (Fig. 4N) and its increased recruitment to E-cadherin junctions. Indeed, the stabilization of E-cadherin junctions in cytodifferentiated glands is likely to occur through the recruitment of γ-catenin, and possibly involve the ability of this catenin to link cadherin junctions to the intermediate filament cytoskeleton (Leonard et al., 2008).

Roles of E-cadherin in SMG Branching Morphogenesis

Partial silencing of E-cadherin with siRNA inhibits branching morphogenesis and results in aberrantly dilated lumens—To identify the functions of E-cadherin during SMG morphogenesis, we partially inhibited E-cadherin expression using an siRNA strategy. Transfection of E12.5 SMGs with E-cadherin siRNA resulted in a 30% reduction of E-cadherin transcript levels compared to a non-silencing control siRNA (Fig. 7A). This corresponded to a 20% decrease in E-cadherin protein abundance (data not shown). Non-silencing control siRNAs had no effect on either E-cadherin expression or SMG morphogenesis. E-cadherin siRNA inhibited branching morphogenesis by affecting bud formation, gland size, and duct development (Fig. 7B). Partial knockdown of E-cadherin left the peripheral SMG cell layer unaffected (data not shown), while the developing ducts exhibited dilated regions delineated by prominent F-actin staining (Fig. 7Cd). Some of these lumenizing structures were found to contain pockets of pycnotic nuclei (Fig. 7Ce). Thus, a 30% reduction of E-cadherin expression was sufficient to cause detectable defects in SMG morphogenesis. These results suggested that E-cadherin was required for proper lumen formation and branching morphogenesis in the developing SMG.

Inhibition of E-cadherin with a function blocking antibody reveals its role in the survival of ductal cells—Since siRNA impacts E-cadherin expression on a transcriptional level, detection of its consequences on E-cadherin protein abundance depends on the time for the de novo synthesized E-cadherin to reach the cell surface and on its turnover time. Thus, we sought to perturb E-cadherin function in a more immediate manner with an E-cadherin function blocking antibody. The structural unit of E-cadherin involved in cell– cell adhesion consists of five tandemly arranged ectodomains 1 through 5 (EC1–EC5) (Fig. 8A), which in the presence of Ca^{23} exist as protease-resistant elongated rod-like structures that associate to form parallel *cis* dimers. We first tested whether inhibition of E-cadherin function using a function blocking antibody that targets the EC5 ectodomain (Ozawa et al., 1991) affected branching morphogenesis. The function blocking antibody was added at experimentally selected concentrations (see Experimental Procedures section) to E13.5 SMG ex vivo cultures. Incubation of E13.5 SMGs with control antibodies that included nonimmune rat IgG and an antibody to the cytoplasmic domain of E-cadherin did not affect branching morphogenesis or the structural morphology of the gland (Fig. 8B,a,b). Incubation of SMGs with the EC5 function blocking antibody resulted in a 65% reduction of bud formation (Fig. 8B,d). Also, the EC5 antibody had a pronounced inhibitory effect on the size of the glands (Fig. 8B,c). These data confirmed the siRNA results that E-cadherin functioned in SMG branching morphogenesis.

To assure that the function blocking antibody targeted E-cadherin junctions throughout the gland, E13.5 SMGs grown in the presence of the EC5 antibody were fixed and then labeled with FITC-conjugated secondary antibodies. As shown in Figure 8C, the antibody to EC5 was uniformly distributed at the lateral borders of cells at the buds' periphery and in the interior. In addition, immunostaining for β-catenin in the antibody-treated glands showed that it was

still present at lateral cell borders targeted by the E-cadherin antibody (data not shown). Thus, the function blocking antibody was able to access all cells within the SMG but it did not appear to disrupt all the existing adherens junctions, consistent with the finding reported for MDCK cells (Capaldo and Macara, 2007). To determine whether EC5 treatment altered cadherin complex stability, we examined the Triton solubility of E-cadherin. We detected no change in E-cadherin Triton insolubility between control and EC5-treated SMGs (Fig. 8D), consistent with the continued presence of β-catenin at cell– cell interfaces. Although E-cadherin complex stability was unaffected, there was a 42% reduction in E-cadherin expression levels in response to EC5 treatment (Fig. 8E). The latter most likely reflected the loss of ductal structures (see below).

To further evaluate the morphological consequences of the EC5-mediated inhibition of E-cadherin function, we carried out histological analysis of hematoxylin and eosin-stained (H&E) serial sections of IgG- and EC5-treated SMGs. While the IgG controls exhibited characteristic structural features consisting of terminal buds and ducts, SMGs incubated in the presence of the EC5 antibody displayed aberrantly dilated lumens that extended into the terminal buds (Fig. 9A, unfilled arrows). The incidence of dilated ducts was >90% for the samples examined, and was most prominent at sites where the newly developing ducts extended into the terminal bud regions. These results confirmed our observations with E-cadherin siRNA and provided further evidence that E-cadherin was required for normal lumenization of ducts during SMG morphogenesis.

As shown in Figure 5, when ductal precursors undergo differentiation into duct cells they acquire prominent E-cadherin junctions at their apical lateral borders. Since E-cadherin has been shown to signal cell survival, we investigated whether aberrant dilation of lumens in EC5-treated SMGs was caused by inappropriate death of differentiating duct cells. First, we examined F-actin distribution and nuclear staining in SMGs treated with the E-cadherin function blocking antibody against EC5. Compared to IgG-treated controls, no significant changes in morphology were detected in cells comprising the outer layer or in the adjacent proliferating ductal precursors (Fig. 9B). The finding that the outer layer was not disrupted by EC5 treatment suggested that there might be another cadherin expressed in this region of the embryonic SMG. To examine the possibility that another cadherin junction co-existed with E-cadherin in the outer layer, we immunostained E12.5 SMGs with antibody to N-cadherin and examined them by confocal microscopy. N-cadherin was expressed in the early SMG and appeared to be most highly localized to the outer layer (Supp. Fig. 4).

In contrast to the outer cell layer, exposure of the early embryonic SMG to the EC5 function blocking antibody caused disorganization of differentiating duct cells and led to the formation of large hollow areas delineated by prominent F-actin staining in the cells lining these luminal structures (Fig. 9B, d). These areas were filled with pycnotic nuclei, a likely consequence of apoptotic cell death in response to the inhibition of E-cadherin function (Fig. 9B,e dotted outline). In contrast, in non-immune IgG-treated glands only a few pycnotic nuclei were detected within newly formed lumens of the developing ducts (Fig. 9B, b,c), consistent with previous studies that demonstrated that lumen formation during SMG development involves apoptosis (Melnick and Jaskoll, 2000; Tucker, 2007). We note that there was variation in the numbers of buds and regions in which the pycnotic nuclei were detected following the treatment with EC5 antibody, suggesting that this effect was developmental-stage sensitive.

To confirm that E-cadherin was essential for the survival of differentiating duct cells, we immunostained control and EC5-treated SMGs with an antibody to cleaved caspase 3, a marker for cells undergoing apoptosis. EC5-treated SMGs cultured for 42 hr displayed aberrantly dilated lumens with prominent staining for cleaved caspase 3, indicating that they were formed by inappropriate activation of apoptotic cell death pathways in maturing ductal cells (Fig. 9C).

By 48 hr, when significant dilation of lumens had already occurred, caspase 3 staining was still detected in regions where the newly formed ducts extended into terminal buds, indicating that aberrant lumenization of ducts was driven by apoptosis as a consequence of inhibition of E-cadherin function (data not shown). Cell death was further confirmed by positive TUNEL staining in the dilated lumens of tissue sections from EC5-treated SMGs (data not shown). We conclude that E-cadherin function was required for stabilization of E-cadherin junctions that, in turn, were critical for the survival of these cells during lumenization of ducts.

DISCUSSION

The SMG belongs to epithelial tissues, including the lung, kidney, and mammary gland, which develop from a single epithelial bud through branching morphogenesis. The latter is a complex developmental process that involves reciprocal signaling among different cell types, changes in gene expression patterns, dynamic reorganization and movements of cells, remodeling of the basement membrane, temporal and spatial engagement of numerous signaling pathways, all of which converge to regulate growth, branching, and duct formation (Hogan, 2006; Kerman et al., 2006; Patel et al., 2006). Although the E-cadherin adhesion receptor has an acknowledged function in epithelial branching morphogenesis, relatively little is known of how in addition to mediating intercellular adhesion E-cadherin impacts the development of acini and ducts. In this report we present evidence that during SMG embryonic development, acinar and ductal cell fates are determined already at a single bud stage and that E-cadherin junctions play pivotal and distinct roles in their organization into mature structures.

Similar to a previous report, which suggested that the initial bud consisted of disorganized cells with E-cadherin and β-catenin uniformly and diffusely distributed over their surface (Hieda et al., 1996; Heida and Nakanishi, 1997), we found disorganized cells in the interior of the early SMG buds. However, our studies also show that the initial SMG bud contains another cell population in the outer layer in contact with the basement membrane. This cell population has columnar morphology with distinct E-cadherin junctions. The molecular mechanisms underlying the critical role of E-cadherin adhesion in the initiation of epithelial cell polarity have been recently described (Nejsum and Nelson, 2007). Thus, the presence of organized E-cadherin junctions in the outer columnar cells is likely to be linked to their columnar morphology. Our studies also show that following clefting and growth of the initial bud, these organized peripheral cells are maintained in, and restricted to, the outer cell layer of the newly formed end-buds. Inhibition of E-cadherin with either siRNA or function blocking antibody demonstrated that E-cadherin junctions were required for branching morphogenesis. One possible explanation is that E-cadherin junctions in the peripheral cell layer were required for branching and new bud formation. In these studies, however, the morphology of the outer cell layer remained unaffected. It is possible that in the absence of E-cadherin function, the morphology of the outer cells was maintained by N-cadherin junctions, which were highly expressed in these cells. It is also possible that the observed effects of inhibition of E-cadherin on the SMG outgrowth and budding were influenced by the defective duct formation.

The presence of two morphologically distinct cell populations was reported previously but not until a later point in SMG morphogenesis, at E13.5 or the pseudoglandular stage, using an EM approach (Kadoya and Yamashina, 1989, 1993, 2005; Kadoya et al., 1995). Further evidence for the existence of two distinct cell populations within terminal end-buds at the pseudoglandular stage was obtained from studies of cell migration behavior in which cells in contact with the basement membrane were shown to move and travel differently from the interior cells (Larsen et al., 2006). Moreover, cells in the interior of the bud could become integrated into the outer layer, further emphasizing the dynamic nature of the terminal buds during SMG development (Larsen et al., 2006).

Our studies are the first to provide evidence that the peripheral columnar cells with organized E-cadherin/β-catenin junctions were destined for acinar cell fate. Immunofluorescence analyses showed that as early as E13.5, only cells in the outer layer expressed the neonatal acinar cell marker B1. Western blot studies showed that B1 was detected by E13.5, which follows the initial bud stage, suggesting that the peripheral cells of the initial SMG bud were acinar precursors. Importantly, the B1-positive outer cell layer was maintained during branching and growth of the SMG, through the formation of acini in the cytodifferentiated E18.5 SMG. Our identification of cells in the outer layer as cells expressing the neonatal acinar marker B1 much before acinar structures are formed is novel and suggests that we have identified acinar precursors.

While cells committed to the acinar lineage were restricted to the outer cell layer throughout SMG embryonic development and eventually formed the acini, cells in the interior of the bud formed the duct system. The initial organization of these ducts was identified as early as E13.5 as a group of cells aligned along the proximal-distal axis with prominent F-actin filaments and expressing the cytokeratin ductal marker K7. Moreover, this initial organization of ductal precursors preceded the acquisition of defined E-cadherin junctions in these cells. Well-defined E-cadherin junctions were first detected at the apical-lateral borders of cells that lined the ducts and appeared coincident with lumen formation. The latter was also associated with the detection of ZO-1 at sites apical to E-cadherin junctions, suggesting that these cells had tight junctions. Therefore, less organized E-cadherin in the interior bud cells may be critical to allow cellular rearrangements during initial duct formation. Once ductal lumens are formed, E-cadherin junctions may be required to stabilize ductal structures.

Apoptosis has been shown be involved in normal lumen formation of the SMG and other glandular tissues (Melnick and Jaskoll, 2000; Mailleux et al., 2007). Our functional studies with E-cadherin siRNA and EC5 function blocking antibody demonstrate the protective role of E-cadherin junctions in the epithelial cells that will line the lumen of the newly formed ducts during the lumenization process. Both approaches blocked the formation of E-cadherin junctions in the duct cells that resulted in aberrantly dilated luminal spaces. The detection of numerous pycnotic nuclei and cleaved caspase 3 in these lumens provided evidence that the expanded lumens arose due to inappropriate apoptosis of duct cells. Thus, E-cadherin junctions provide a survival signal to the maturing duct cells. A similar effect of E-cadherin on cell survival was shown in the Drosophila salivary gland where inappropriate loss of β-catenin and E-cadherin caused by expression of constitutively active $Rac1V^{12}$ induced cell death (Pirraglia et al., 2006). Furthermore, in the absence of p120 catenin, a stabilizing partner of E-cadherin, mouse SMGs displayed aberrantly dilated lumens (Davis and Reynolds, 2006). In other tissues, such as mammary gland and skin, E-cadherin has also been shown to promote cell survival (Boussadia et al., 2002; Tinkle et al., 2003).

Collectively, our studies show that two distinct cell populations are present in the SMG from the single bud stage. We demonstrate for the first time that the cell population in the outer layer contains precursors of acinar cells that go on to form the acinar structures of cytodifferentiated gland. The second population, the cells in the interior bud regions, reorganizes to form ducts. Both of these populations have E-cadherin junctions, although their organization during development is different. Interfering with E-cadherin function has major effects on the development of the SMG, blocking its outgrowth, bud formation, and causing dilation of ducts due to the loss of protection of the luminal epithelium. Future studies will focus on additional functions of E-cadherin junctions during SMG development, particularly their role in mechanotransduction events during duct formation and morphogenesis of the gland (Lecuit and Lenne, 2007). These cadherin functions are likely important in the formation of cell boundaries and cellular rearrangements critical to the formation of acinar and ductal structures.

EXPERIMENTAL PROCEDURES

SMG Organ Cultures

Animal experiments were approved by the Institutional Animal Care and Use Committee (IACUC) at the Boston University Medical Center. Sub-mandibular/sublingual salivary gland rudiments (Hoffman et al., 2002) were dissected from E12.5–E18.5 CD-1 or ICR mice and cultured on Whatman Nuclepore Tracketch filters, at the air/medium interface at 37°C in a humidified 5% CO_2 atmosphere. The filters were floated in 200 μl of DMEM/F12, supplemented with 100 U/ml penicillin, 100 μg/ml streptomycin, 150 μg/ml vitamin C, and 50 μg/ml transferrin, in 50-mm glass-bottom microwell dishes (MatTek, Ashland, MA).

RNA Interference

Small interfering RNAs (siRNA) targeting E-cadherin were obtained as SMART-pool™ sequences from Dharmacon. Non-silencing negative control siRNA was purchased from Qiagen. The efficiency of transfections was determined to be 98% using off-target Cy3-siRNA (Dharmacon). To determine optimal conditions for siRNA-mediated partial inhibition of E-cadherin expression, concentrations of siRNA ranging from 50 to 400 nM were initially tested for various periods of time that included 12, 24, 36, 48, and 72 hr. The most pronounced effects on SMG branching morphogenesis were detected between 22 and 48 hr with 200 nM siRNA. Concentrations below 200 nM did not show discernable inhibition of branching morphogenesis, while 400 nM had consequences similar to 200 nM. After 72 hr of siRNA treatment, inhibition of branching morphogenesis was alleviated, suggesting that the effect of siRNA was reversible. Therefore, we elected to use 200 nM siRNA for a period between 22–48 hr to partially inhibit E-cadherin expression, Twelve E12.5 SMGs (six glands/filter) were transfected with either 200 nM E-cadherin siRNA or with a non-silencing control siRNA using RNAiFect (Qiagen). Each embryo served as a source of one SMG for siRNA and one for a non-silencing control. Transfected SMGs were grown for 22–48 hr and processed for RT-PCR analyses to measure gene knockdown. Total RNAs were purified and used for cDNA synthesis to assess E-cadherin gene expression by real-time PCR. The gene expression profiles were generated by normalizing the Ct (threshold cycle numbers) of E-cadherin with a housekeeping gene 29S and by comparing the gene expression of SMGs treated with non-silencing (NS) and silencing (S) E-cadherin siRNAs. Statistical analysis was performed using real-time PCR from three independent RNA preparations.

Function Blocking Antibody

The E-cadherin function blocking antibody targeting the EC5 ectodomain was used at 100 μg/ml. This concentration was determined based on the dose- and time-dependence studies. The dose selected had no further phenotypic consequences either at higher concentrations or longer incubation times. For inhibition studies, E13.5 SMGs were cultured for 2 hr prior to addition of function blocking antibodies, followed by incubation in the presence of function blocking antibodies for 48 hr. Typically, twelve SMGs from two litters were used for one experiment (six SMGs per filter), with each embryo serving as a source of one SMG for the function blocking antibody and one for the control IgG incubation. Bright-field images were collected 2, 24, and 48 hr following treatment on a Nikon Eclipse TS100 (4×/0.13) microscope equipped with Nikon E5400 camera. The buds were counted and the data were tabulated by MetaMorph (Universal Imaging Corporation, Downington, PA; V6.2). Statistical analysis was tabulated using PRISM software (Graph Software Inc., San Diego, CA; V4.0).

Tissue Extraction and Protein Determination

Isolated SMGs were either immediately frozen on dry ice or they were grown on filters, as indicated. For the preparation of total tissue lysates, SMGs were extracted in OGT buffer (1%

Triton X-100, 45 mM n-Octyl β-D glucopyranoside in a buffer containing 100 mM NaCl, 1 mM $MgCl_2$, 5 mM EDTA, 10 mM imidazole, 3 mM sodium pyrophosphate, 50 mM sodium fluoride, 1 mM sodium vanadate, and a protease inhibitor cocktail (Sigma)).

For determination of Triton solubility/insolubility as a measure of degree of cytoskeletal association of SMG proteins, tissues were extracted with Triton extraction buffer (1% Triton X-100 in a buffer containing 100 mM NaCl, 1 mM $MgCl_2$, 5 mM EDTA, 10 mM imidazole, 3 mM sodium pyrophosphate, 50 mM sodium fluoride, 1 mM sodium vanadate, and a protease inhibitor cocktail (Sigma) at 4°C. The Triton-soluble and -insoluble fractions were separated by centrifugation at 12,000*g* for 10 min. The resulting Triton-insoluble pellet was re-extracted with OGT buffer. Protein concentration was determined by the BCA assay.

Antibodies and Stains

Antibodies to E-cadherin, β-catenin, γ-catenin, α-catenin, N-cadherin, and Ki67 were obtained from BD Transduction. Antibody specific for β-actin and function blocking antibody (clone DECMA-1) specific for E-cadherin ectodomain EC5 were obtained from Sigma Aldrich. Antibody to cytokeratin 7 (K7) was purchased from AbCam and to ZO-1 from Zymed. Antibody to cleaved caspase-3 was from Cell Signaling and to aquaporin 5 (AQP5) from Alpha Diagnostic International. Antibody to heparan sulfate proteoglycan, perlecan, (clone A7L6) was from Chemicon. Anti-B1 antibodies were a gift from Lily Mirels, UC Berkeley. Rhodamine-conjugated phalloidin and monomeric cyanine nucleic acid stain were purchased from Molecular Probes. Secondary antibodies conjugated to horseradish peroxidase were from Bio Rad, and AffiniPure goat anti-mouse and goat anti-rabbit IgG Fab fragments were from either Jackson ImmunoResearch Laboratories or Molecular Probes. Purified rat IgG was purchased from BD Biosciences.

Histology

For histological analysis, four E13.5 SMGs, cultured in the presence of either IgG or function blocking antibody to EC5 for 48 hr, were fixed in 4%paraformaldehyde in PBS and dehydrated. Samples were embedded in paraffin, cut (8-μm sections) and stained with hematoxylin and eosin at the Harvard Core Facility (Beth Israel Deaconess Medical Center). Digital images of light microscopy were acquired with a TE 300 microscope (Nikon).

Immunoprecipitation

For each independent study, protein extracts, ranging from 80–350 μg, were used. Protein extracts were prepared from 16 to 70 E13.5 SMGs pooled from two to nine litters and from four E18.5 SMGs pooled from one litter. E-cadherin was immunoprecipitated by sequential incubation for 1 hr with a monoclonal antibody to E-cadherin followed by Mouse True Blot IP beads 4°C (1 hr incubation) (eBioscience, San Diego, CA) as described previously (Walker and Menko, 1999; Walker et al., 2002).

Immunoblots

For each Western blot analysis, including Triton solubility determination, between eight and ten E13.5 SMGs from one litter and two E18.5 SMGs from one litter, were pooled and used for protein extraction, as described above. Proteins were separated on 4–12% Trisglycine gels obtained from Novex, electrophoretically transferred to Immobilon-P membrane (Millipore Corp., Bedford, MA) and immunoblotted as described previously. For immunoblot analyses, whole tissue lysates were routinely loaded at 10–15 μg of total protein. For immunoblot analyses of Triton-soluble fractions, samples were loaded at equal protein concentrations (10–15 μg). Their respective insoluble fractions were loaded at volumes equal to the soluble fractions so that direct comparisons could be made. All gels were run under reducing

conditions. For detection, ECL or ECL plus reagents from Amersham Life Sciences were used. Immunoblots were scanned and densitometry analysis performed using Kodak 1D software. To assure that quantification was performed in the linear range, blots were subject to multiple exposures.

Immunofluorescence

For whole mount immunofluorescence, dissected E12.5 and E13.5 SMGs were grown on filters overnight, while E15.5 and E18.5 SMGs were grown on filters for 2 hr, prior to processing for immunostaining with specific antibodies. Typically, each immunofluorescence localization study included two filters with six SMGs from one litter each. SMGs were fixed with 3.7% paraformaldehyde for 2 hr, washed with PBS, and permeabilized with 0.1% Triton X-100 for 15 min at room temperature. For α-catenin immunostaining, tissues were fixed with ice-cold acetone/methanol (1:1) for 15 min on ice, and washed with PBS. Glands were blocked overnight at 4°C with 10% donkey serum, and 1% BSA in PBS-Tween 20 (0.1%) and incubated with primary antibodies for 4–6 hr at RT, followed by secondary antibodies, either donkey or goat F(ab)2 fragments labeled with fluorescein (Molecular Probes, Eugene, OR), for 1 hr. Phalloidin conjugated to an alternate fluorochrome was added for 30 min, and nuclei were visualized with monomeric cyanine nucleic acid stain. The immunostained samples were analyzed with a Zeiss confocal laser scanning microscope LSM510 META for visualization of individual optical sections and the generation of Z-stacks of optical planes that crossed the entire gland using LSM510-expert mode acquisition software. To trace the interior presumptive ductal cells, detailed confocal analyses of Z-stacks with optical slices as thin as 0.1 μm were analyzed. To insure valid comparison of fluorescence intensities between samples within a particular study, settings were fixed to the most highly stained sample and all other images were acquired at those settings.

Acknowledgments

Grant Sponser: NIH; Grant numbers: DE014437, DE010183, EY014798.

We thank Wellington Cardoso for helpful discussions and Mihai Nita-Lazar, Donna Afshar, and Michele Leonard for a critical reading of the manuscript. The authors also thank Ni Zhai for her technical assistance with the confocal imaging. This work was supported by Grants DE14437 and DE10183 from the NIH/NIDCR to M.A.K. and EY014798 to A.S.M.

References

Ball WD, Mirels L, Hand AR. Psp and Smgb: a model for developmental and functional regulation in the rat major salivary glands. Biochem Soc Trans 2003;31:777–780. [PubMed: 12887304]

Benjamin JM, Nelson WJ. Bench to bedside and back again: molecular mechanisms of alpha-catenin function and roles in tumorigenesis. Semin Cancer Biol 2008;18:53– 64. [PubMed: 17945508]

Bernfield M, Danerjee SD, Koda JE, Rapraeger AC. Remodelling of the basement membrane: morphogenesis and maturation. Ciba Found Symp 1984;108:179–196. [PubMed: 6569828]

Boussadia O, Kutsch S, Hierholzer A, Delmas V, Kemler R. E-cadherin is a survival factor for the lactating mouse mammary gland. Mech Dev 2002;115:53– 62. [PubMed: 12049767]

Capaldo CT, Macara IG. Depletion of E-cadherin disrupts establishment but not maintenence of cell junctions in Madin-Darby canine kidney epithelial cells. Mol Biol Cell 2007;18:189 –200. [PubMed: 17093058]

Cowin P, Burke B. Cytoskeleton-membrane interactions. Curr Opin Cell Biol 1996;8:56 – 65. [PubMed: 8791403]

Cowin P, Kapprella H-P, Franke WW, Tamkun J, Hynes RO. Plakoglobin: a protein common to different kinds of intercellular adhering junctions. Cell 1986;46:1063–1073. [PubMed: 3530498]

Davis MA, Reynolds AB. Blocked acinar development, E-cadherin reduction, and intraepithelial neoplasia upon ablation of p120-catenin in the mouse salivary gland. Dev Cell 2006;10:21–31. [PubMed: 16399075]

Denny PC, Ball WD, Redman RS. Salivary glands: a paradigm for diversity of gland development. Crit Rev Oral Biol Med 1997;8:51–55. [PubMed: 9063625]

Fernandes RP, Cotanche DA, Lennon-Hopkins K, Erkan F, Menko AS, Kukuruzinska MA. Differential expression of proliferative, cytoskeletal, and adhesive proteins during postnatal development of the hamster submandibular gland. Histochem Cell Biol 1999;111:153–162. [PubMed: 10090576]

Grunwald GB. The structural and functional analysis of cadherin calcium-dependent cell adhesion molecules. Curr Opin Cell Biol 1993;5:797– 805. [PubMed: 8240823]

Gumbiner BM. Cell adhesion: the molecular basis of tissue architercture and morphogenesis. Cell 1996;84:345–357. [PubMed: 8608588]

Gumbiner BM. Regulation of cadherin-mediated adhesion in morphogenesis. Nat Rev Mol Cell Biol 2005;6:622– 634. [PubMed: 16025097]

Halbleib JM, Nelson WJ. Cadherins in development: cell adhesion, sorting and tissue morphogenesis. Genes Dev 2006;20:3199 –3214. [PubMed: 17158740]

Hartsock A, Nelson WJ. Adherens and tight junctions: Structure, function and connections to the actin cytoskeleton. Biochim Biophys Acta 2008;1778:660 – 669. [PubMed: 17854762]

Heida Y, Nakanishi Y. Epithelial morphogenesis in mouse embryonic sub-mandibular gland: its relationships to the tissue organization of epithelium and mesenchyme. Dev Growth Differ 1997;39:1– 8. [PubMed: 9079029]

Hieda Y, Iwai K, Morita T, Nakanishi Y. Mouse embryonic submandibular gland epithelium loses its tissue integrity during early branching morphogenesis. Dev Dyn 1996;207:395– 403. [PubMed: 8950514]

Hirano S, Nose A, Hatta K, Kawakami A, Takeichi M. Calcium-dependent cell-cell adhesion molecules (cadherins): specificities and possible involvement of actin bundles. J Cell Biol 1987;105:2501–2511. [PubMed: 3320048]

Hoffman MP, Kidder BL, Steinberg ZL, Lakhani S, Ho S, Kleinman HK, Larsen M. Gene expression profiles of mouse submandibular gland development: FGFR1 regulates branching morphogenesis in vitro through BMP- and FGF-dependent mechanisms. Development 2002;129:5767–5778. [PubMed: 12421715]

Hogan BL. Building organs from buds, branches and tubes. Differentiation 2006;74:323–325. [PubMed: 16916372]

Jamora C, Fuchs E. Intercellular adhesion, signalling and the cytoskeleton. Nat Cell Biol 2002;4:101–108.

Jaskoll T, Melnick M. Submindibular gland morphogenesis: stage-specific expression of TGF-a/EGF, IGF, TGF-b, TNF, and IL-6 signal transduction in normal embryonic mice and the phenotypic effects of TGF-b2, TGF-b-3, and EGF-R null mutations. Anat Rec 1999;256:252–268. [PubMed: 10521784]

Kadoya Y, Yamashina S. Intracellular accumulation of basement membrane components during morphogenesis of rat submandibular gland. J Histochem Cytochem 1989;37:1387–1392. [PubMed: 2768808]

Kadoya Y, Yamashina S. Distribution of alpha 6 integrin subunit in developing mouse submandibular gland. J Histochem Cytochem 1993;41:1707–1714. [PubMed: 8409377]

Kadoya Y, Yamashina S. Salivary gland morphogenesis and basement membranes. Anat Sci Int 2005;80:71–79. [PubMed: 15960312]

Kadoya Y, Kadoya K, Durbeej M, Holmvall K, Sorokin L, Ekblom P. Antibodies against domain E3 of laminin-1 and integrin alpha 6 subunit perturb branching epithelial morphogenesis of submandibular gland, but by different modes. J Cell Biol 1995;129:521–534. [PubMed: 7536749]

Kashimata M, Sayeed S, Ka A, Onetti-Muda A, Sakagami H, Faraggiana T, Gresik EW. The ERK-1/2 signaling pathway is involved in the stimulation of branching morphogenesis of fetal mouse submandibular glands by EGF. Dev Biol 2000;220:183–196. [PubMed: 10753509]

Kerman BE, Cheshire AM, Andrew DJ. From fate to function: the Drosophila trachea and salivary gland as models for tubulogenesis. Differentiation 2006;74:326 –348. [PubMed: 16916373]

Kobielak A, Fuchs E. alpha-Catenin: at the junction of intercellular adhesion and actin dynamics. Nature Rev 2004;5:614 –623.

Larsen M, Wei C, Yamada KM. Cell and fibronectin dynamics during branching morphogenesis. J Cell Sci 2006;119:3376 –3384. [PubMed: 16882689]

Lecuit T, Lenne PF. Cell surface mechanics and the control of cell shape, tissue patterns and morphogenesis. Nat Rev Mol Cell Biol 2007;8:633– 644. [PubMed: 17643125]

Leonard M, Chan Y, Menko AS. Identification of a novel intermediate filament-linked N-cadherin/gamma-catenin complex involved in the establishement of the cytoarchitecture of differentiated lens fiber cells. Dev Biol 2008;319:298 –308. [PubMed: 18514185]

Mailleux AA, Overholtzer M, Schmelzle T, Bouillet P, Strasser A, Brugge JS. BIM regulates apoptosis during mammary ductal morphogenesis, and its absence reveals alternative cell death mechanisms. Dev Cell 2007;12:221–234. [PubMed: 17276340]

Marrs JA, Nelson WJ. Cadherin cell adhesion molecules in differentiation and embryogenesis. Int Rev Cytol 1996;165:159 –205. [PubMed: 8900959]

Melnick M, Jaskoll T. Mouse sub-mandibular gland morphogenesis: a paradigm for embryonic signal processing. Crit Rev Oral Biol Med 2000;11:199 –215. [PubMed: 12002815]

Menko AS, Zhang L, Schiano F, Kreidberg JA, Kukuruzinska MA. Regulation of cadherin junctions during mouse sub-mandibular gland development. Dev Dyn 2002;224:321–333. [PubMed: 12112462]

Mirels L, Miranda AJ, Ball WD. Characterization of the rat salivary-gland B1-immunoreactive proteins. Biochem J 1998;330:437– 444. [PubMed: 9461541]

Nakagawa S, Takeichi M. Neural crest cell-cell adhesion controlled by sequential and subpopulation-specific expression of novel cadherins. Development 1995;121:1321–1332. [PubMed: 7540531]

Nejsum LN, Nelson WJ. A molecular mechanism directly linking E-cadherin adhesion to initiation of epithelial cell surface polarity. J Cell Biol 2007;178:323–335. [PubMed: 17635938]

Ozawa M, Hoschutzky H, Herrenknecht K, Kemler R. A possible new adhesive site in the cell-adhesion molecule unvomorulin. Mech Dev 1991;33:49 –56. [PubMed: 1710917]

Patel VN, Rebustini IT, Hoffman MP. Salivary gland branching morphogenesis. Differentiation 2006;74:349 –364. [PubMed: 16916374]

Pirraglia C, Jattani R, Myat MM. Rac function in epithelial tube morphogenesis. Dev Biol 2006;290:435–446. [PubMed: 16412417]

Sakai T, Larsen M, Yamada KM. Fibronectin requirement in branching morphogenesis. Nature 2003;423:876–881. [PubMed: 12815434]

Takeichi M. Cadherin cell adhesion receptors as a morphogenetic regulator. Science 1991;251:1451–1455. [PubMed: 2006419]

Tinkle CL, Lechler T, Pasolli HA, Fuchs E. Conditional targeting of E-cadherin in skin: Insights into hyperproliferative and degenerative responses. Proc Natl Acad Sci 2003;101:552–557. [PubMed: 14704278]

Tucker AS. Salivary gland development. Semin Cell Dev Biol 2007;18:237–244. [PubMed: 17336109]

Walker JL, Menko AS. alpha6 Integrin is regulated with lens cell differentiation by linkage to the cytoskeleton and isoform switching. Dev Biol 1999;210:497–511. [PubMed: 10357906]

Walker JL, Zhang L, Zhou J, Woolkalis MJ, Menko AS. Role for alpha 6 integrin during lens development: Evidence for signaling through IGF-1R and ERK. Dev Dyn 2002;223:273–284. [PubMed: 11836791]

Wei C, Larsen M, Hoffman MP, Yamada KM. Self-organization and branching morphogenesis of primary salivary epithelial cells. Tissue Eng 2007;13:721–735. [PubMed: 17341161]

Wheelock MJ, Johnson KR. Cadherins as modulators of cellular phenotype. Ann Rev Cell Dev Biol 2003;19:207–235. [PubMed: 14570569]

Yamaguchi Y, Yonemura S, Takada S. Grainyhead-related transcription factor is required for duct maturation in the salivary gland and the kidney of the mouse. Development 2006;133:4737– 4748. [PubMed: 17079272]

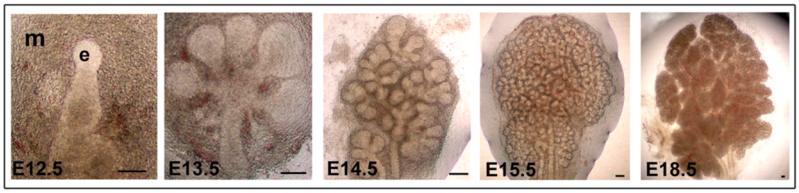

Fig. 1.

Morphogenesis of SMG organ cultures. SMG epithelial buds (*e*), and surrounding mesenchyme (*m*) isolated from embryonic days E12.5 through E18.5 were cultured and observed by phase microscopy. Scale bar = 100 μm.

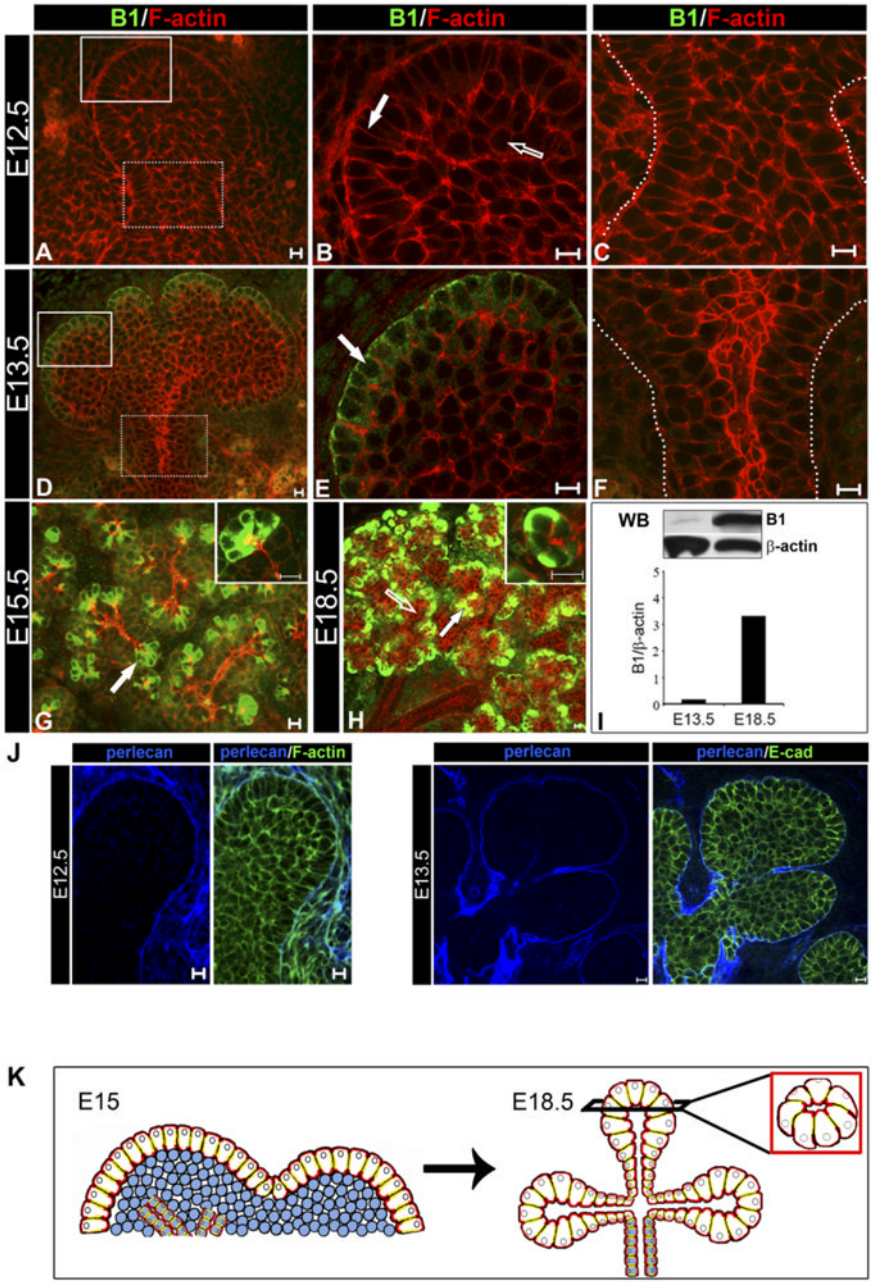

Fig. 2.

The outer cell layer expresses acinar marker, B1, early in SMG bud development. SMGs representing E12.5, E13.5, E15.5, and E18.5 stages of embryonic development were immunostained with anti-B1 antibodies (green), counterstained with rhodamine-phalloidin (red) and examined by confocal microscopy. **A–C:** Cells in the E12.5 SMG were not reactive with B1 antibodies. **D–F:** Immunolocalization of B1 in the E13.5 SMG was restricted to the peripheral cell layer (D, white solid box; E, *block arrow*) while the stalk region was negative (D, white dashed box; F, *region within dashed lines*). **G:** Immunolocalization of B1 in the E15.5 SMGs was maintained in the outer layer of the developing buds (block arrow; inset: 63×). **H:** At E18.5 acinar cells had prominent B1 expression (block arrow; inset: 63×) while ducts remained negative (unfilled arrow). **I:** Expression of B1 was detected early in

morphogenesis and increased in the cytodifferentiated SMG. Glands were extracted with Triton extraction buffer and analyzed by Western blot (WB) using anti-B1 and anti-β-actin antibodies. Bar graph represents B1 normalized to β-actin; shown is one of two independent experiments. **J:** Perlecan staining of the basement membrane of the early SMGs. E12.5 and E13.5 SMGs were immunostained for perlecan (blue) and either E-cadherin (green) or F-actin (green). Perlecan (blue) stains the basement membrane, which is in direct contact with the outer layer of the SMG epithelium. Shown are middle 1-μm optical sections. Scale bar = 10 μm. **K:** A model showing how acinar cell precursors in the outer layer (white cells) develop into acini at the completion of SMG embryonic morphogenesis. Scale bar = 10 μm.

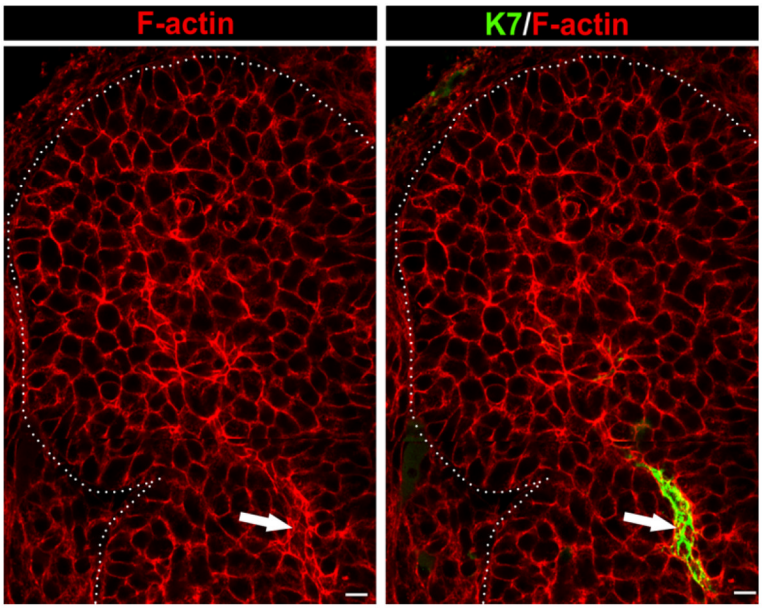

Fig. 3.

Duct formation in the developing SMG. E13.5 glands were immunostained with an antibody to the duct-specific marker, cytokeratin 7 (K7), and counterstained for F-actin with rhodamine-phalloidin (red). Intense regions of F-actin localization overlapped with K7 staining (filled arrows) confirming identification of these actin-rich areas as ductal structures. Scale bar = 10 μm.

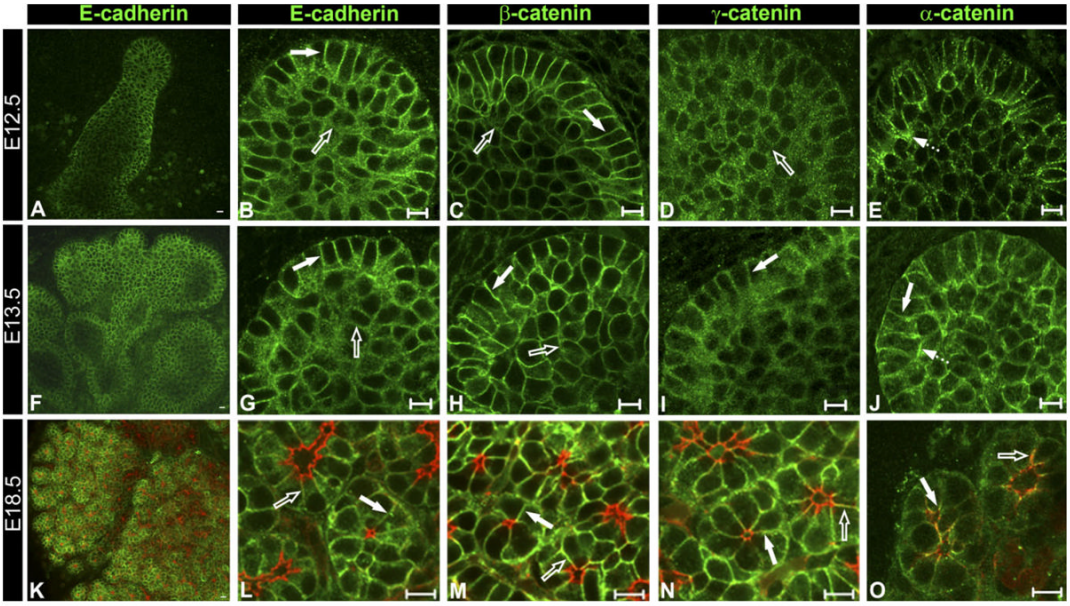

Fig. 4.

Organization of E-cadherin junctions during SMG morphogenesis. SMG buds were immunostained with antibodies to E-cadherin (**A,B, F,G, K,L**), β-catenin (**C,H,M**), γ-catenin (**D,I,N**), and α-catenin (**E,J,O**) and examined by confocal microscopy. Low-power confocal imaging of E-cadherin in E12.5 (A), E13.5 (F), and E18.5 (K) SMGs. High-resolution confocal imaging through the center of the E12.5 buds revealed that E-cadherin and β-catenin were tightly focused at the lateral surfaces of cells at the bud's periphery (B,C, block arrows), while cells in the interior exhibited diffuse staining (B,C, open arrows). γ-catenin staining was diffuse in both the peripheral cells and the cells in the bud's interior (D, open arrow). α-catenin was more intense in the apical domains of the peripheral cells (E, broken arrow). Scale bar = 10 μm. Confocal imaging through the center of E13.5 buds revealed cells with columnar morphology in the outer layer (G–J, block arrows), with E-cadherin and β-catenin tightly focused at the lateral interfaces (G and H, block arrows). The interior regions exhibited more diffuse staining for E-cadherin and β-catenin (G and H, open arrows) than in the peripheral cells. γ-catenin was localized at the lateral borders in the peripheral layer (I, block arrow). α-catenin was detected at the lateral surfaces of cells in the peripheral layer and, prominently, at their apical membranes (J, broken arrow). Scale bar = 10 μm. L–O: E18.5 SMGs were immunostained for E-cadherin, β-catenin, γ-catenin, and α-catenin, counterstained for F-actin with rhodamine-phalloidin (red), and examined by confocal microscopy. Within the acini (block arrows) and ducts (open arrows), E-cadherin, β-catenin, and γ-catenin localized to cell–cell interfaces (L–N, respectively), while α-catenin displayed prominent colocalization with F-actin at the apical domains (O). Scale bar = 10 μm.

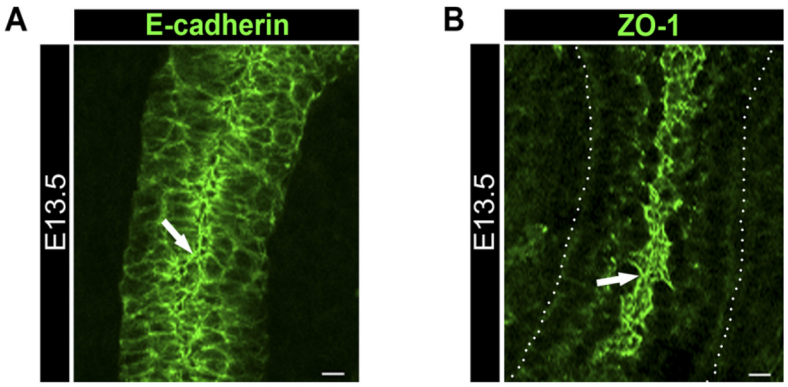

Fig. 5.

Presumptive duct cells have prominent E-cadherin and ZO-1 staining at their apical domains. **A,B:** Confocal imaging of E13.5 glands revealed the distal region of the initial stalk with multilayered cuboidal cells and with focused E-cadherin at the apical and lateral cell borders of the innermost cell layer (A, block arrow) facing the central lumen. B: ZO-1 was detected at the apical cell–cell borders of the presumptive ducts (B, block arrow) facing the central lumen. Scale bar = 10 μm.

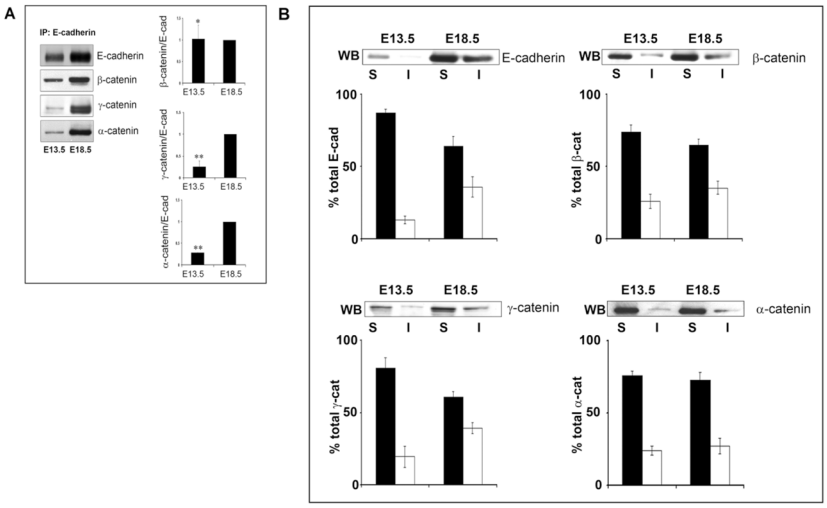

Fig. 6.

SMG development is accompanied by changes in the molecular composition and Triton solubility of E-cadherin junctions. **A:** Total tissue extracts from E13.5 and E18.5 SMGs were immunoprecipitated (IP) with the antibody to E-cadherin and analyzed for association of β-, γ-, and α-catenins by Western blot. While there was little change in β-catenin's association with E-cadherin as the SMG developed, both γ- and α-catenin showed increased interaction from E13.5 to E18.5. Bar graphs reflect E13.5 values normalized to E18.5 for determining the ratio of each catenin in the E-cadherin complex and represent an average of three experiments. Data were normalized to E18.5 values and plotted ± SEM. (*, no significant difference; ***P* < 0.05). **B:** Diminished Triton solubility of E-cadherin and catenins was associated with SMG development. SMGs were extracted with the Triton buffer and Triton-soluble (S) and -insoluble (I) fractions were analyzed by Western blot with antibodies to E-cadherin, β-catenin, γ-catenin, and α-catenin. Bar graphs depicting quantification of the immunoblots are shown (filled bars, Triton-soluble; unfilled bars, Triton-insoluble). E-cadherin, β-catenin, and γ-catenin displayed increased association with the Triton-insoluble fraction in E18.5 SMG compared to early morphogenesis. Little change was observed for α-catenin. Bar graphs represent an average of three independent experiments, except for the γ-catenin data, which was based on two separate studies. Values are plotted as ± SEM.

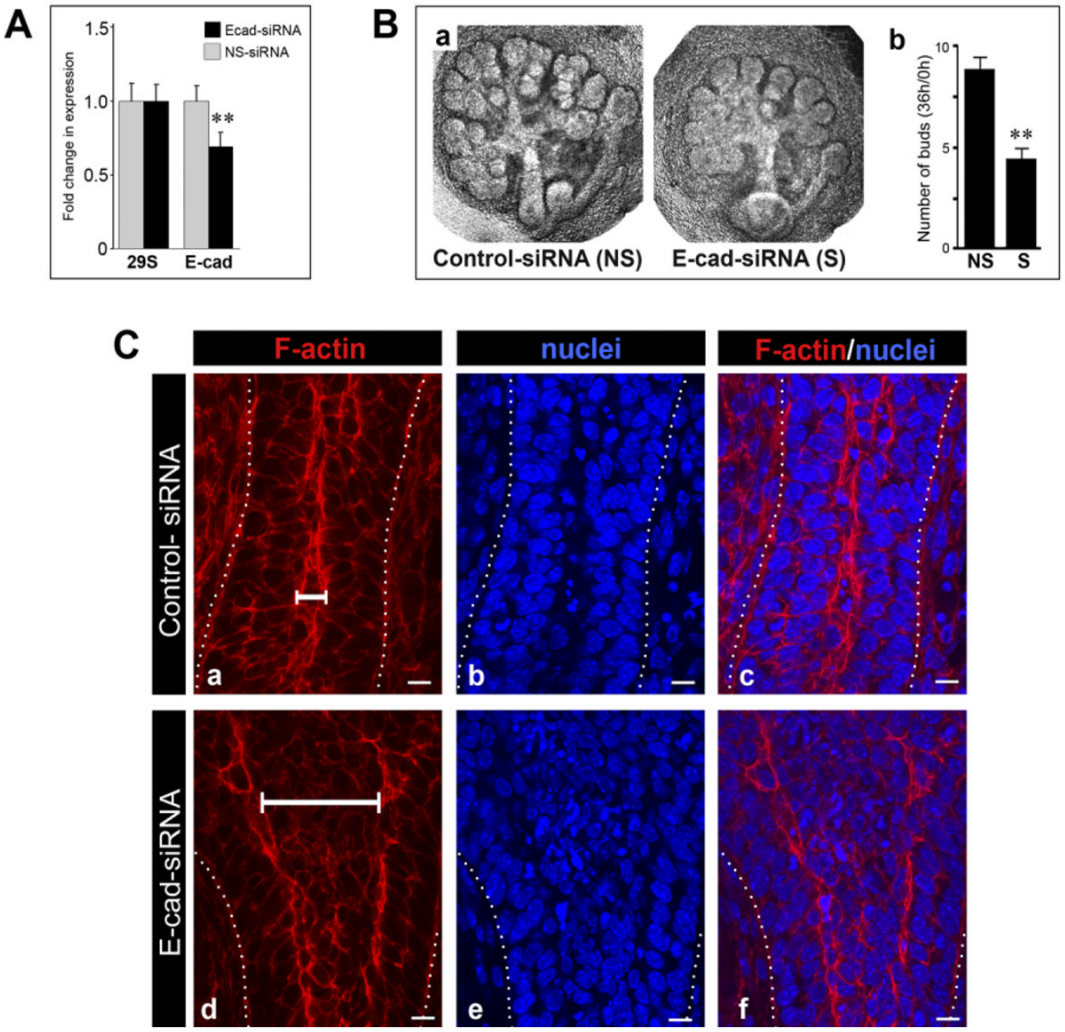

Fig. 7.

Partial inhibition of E-cadherin expression with siRNA interferes with SMG branching morphogenesis and normal duct development. E12.5 SMGs were transfected with either E-cadherin siRNA or with a non-silencing control and grown in culture for 22– 48 hr. **A:** Total RNAs, isolated from SMGs treated with either E-cadherin siRNA or non-silencing controls, were analyzed by real-time PCR and normalized to 29S. Values are expressed as a relative fold change compared to control. E-cadherin mRNA levels were reduced 30% following treatment with E-cadherin siRNA compared to controls. *P* values are unpaired *t*-tests compared to 29S controls, $^{**}P < 0.05$. **B:** Phase microscopy of SMGs transfected with non-silencing (NS) and E-cadherin siRNAs (S) (**a,b**). The number of buds in E-cadherin siRNA-treated glands was reduced by 55% compared to non-silencing controls (**c**) (ANOVA, $^{**}P < 0.05$). **C:** Confocal imaging of F-actin and nuclei of E12 SMGs transfected with either non-silencing control (**a–c**) or E-cadherin siRNA (**d–f**) for 22 hr revealed dilated ducts in the E-cadherin siRNA treated glands (d). Width of ductal lumens is denoted by brackets in a and d). Scale bar = 10 μm.

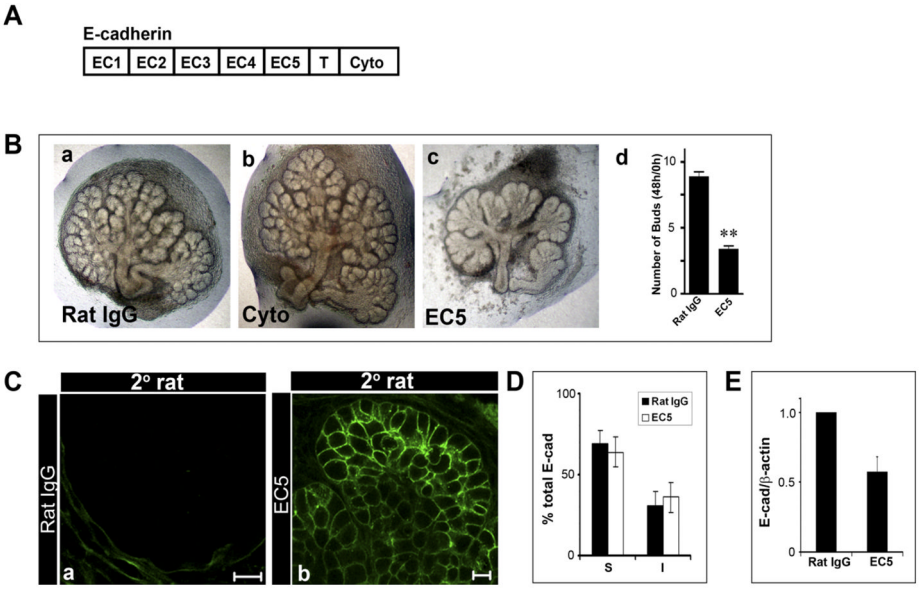

Fig. 8.

E-cadherin junctions are required for branching morphogenesis. **A:** Schematic representation of E-cadherin with five extracellular domains (EC1-EC5), a transmembrane region (T), and an intracellular cytoplasmic domain (Cyto). **B:** Representative phase microscopy of control (a,b) and EC5 function blocking antibody-treated (c) SMG organ cultures. Buds were counted after treatment with the function blocking antibody or Rat IgG and normalized to time zero. A significant decrease (65%) in the number of buds in SMGs treated with the EC5 function blocking antibody (**c,d**) compared to control rat IgG (**a,d**) was detected (ANOVA, $^{**}P < 0.05$). Bar graphs represent one of three independent experiments, with an n = 36. **C:** Organ cultures were incubated with either rat IgG or the function blocking antibody to EC5, stained with FITC-derivatized secondary rat antibodies and analyzed by confocal microscopy. Size bar = 10 μm. **D:** EC5 and rat IgG-treated glands were extracted with Triton buffer and Triton-soluble (S) and -insoluble (I) fractions were analyzed for E-cadherin by Western blot. The bar graph depicts four independent experiments (filled bars, Rat IgG treated; unfilled bars, EC5 treated) with values plotted ± SEM. **E:** SMGs were extracted in Triton extraction buffer and immunoblotted for E-cadherin and β-actin expression. The bar graph depicts the ratio of E-cadherin to β-actin expression with the data normalized to rat IgG and plotted ± SEM.

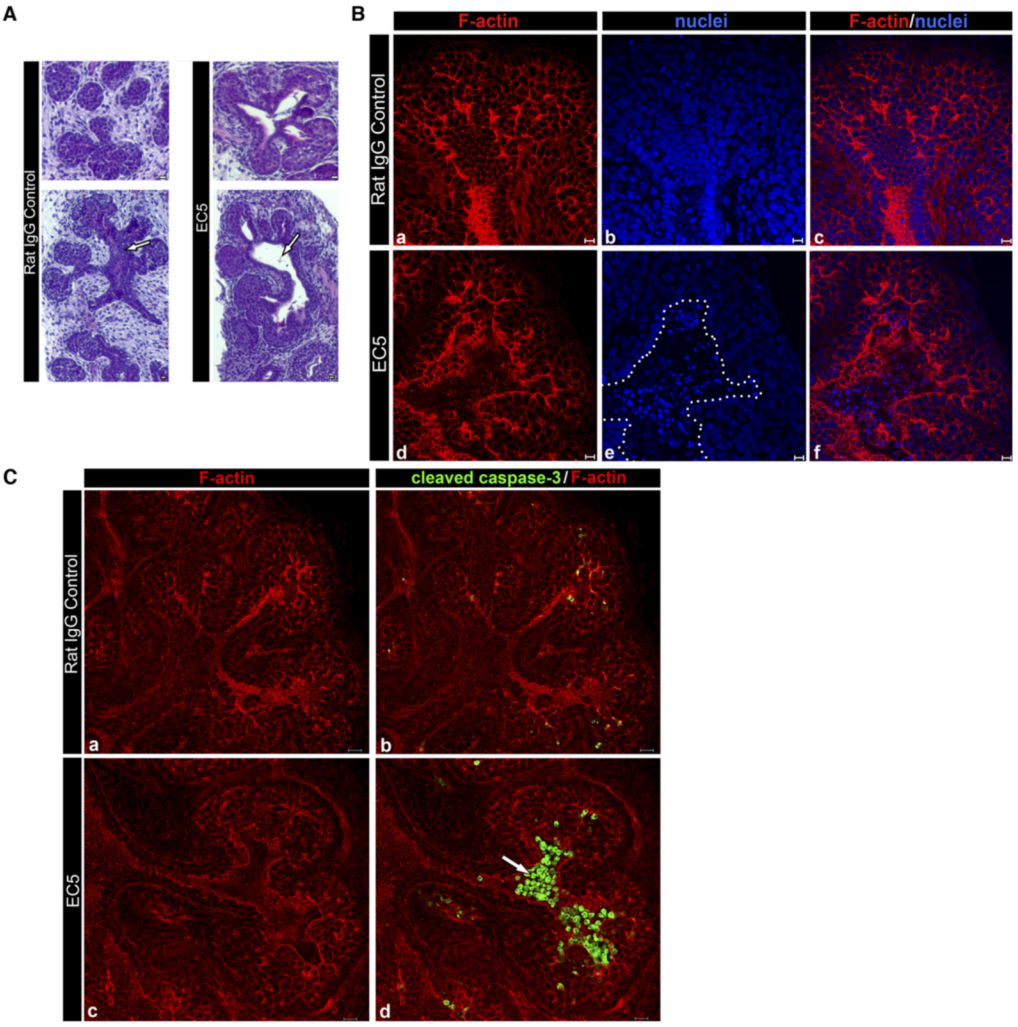

Fig. 9.

Inhibition of E-cadherin with a function blocking antibody to EC5 leads to aberrant dilation of ducts. **A:** E13.5 SMGs were cultured in the presence of either IgG or EC5 function blocking antibody for 48 hr and processed for routine H&E staining. Cross-sections (top) and longitudinal sections (bottom) revealed dilated ductal structures leading to terminal buds in EC5-treated SMGs (block arrow). Scale bar = 10 μm. **B:** Confocal imaging of F-actin and nuclei showed aberrantly large lumens in the EC5-treated SMGs (**d–f**) filled with pycnotic nuclei (e, dashed outline) that were not detected in controls (a–c). Scale bar = 10 μm. **C:** E13.5 SMGs were cultured in the presence of either IgG or EC5 function blocking antibody for 42 hr and immunostained for cleaved caspase 3. Immunofluorescence localization of cleaved caspase 3 revealed prominent staining in the regions of dilated lumens of EC5-treated glands (block arrow). Scale bar = 20 μm.